The fabrication of multicolor electrochromic device based on graphene conductive ink/poly(lactic acid) thin films by voltage-step method

A. BUASRI[a,b,*], S. OJCHARIYAKUL[a], P. KAEWMANECHAI[a], W. EAKVIRIYAPICHAT[a], V. LORYUENYONG[a,b,*]
[a]*Department of Materials Science and Engineering, Faculty of Engineering and Industrial Technology, Silpakorn University, Nakhon Pathom 73000, Thailand*
[b]*Center of Excellence on Petrochemical and Materials Technology, Chulalongkorn University, Bangkok 10330, Thailand*

Today's technology has significantly focused on advanced and smart materials. Electrochromism is a phenomenon wherein the change in optical properties of a material is induced by reversible redox process. Color change usually occurs between colored (darkened) state and transmissive (bleached) states or between two different colored states. In this research, we focused on silver (Ag) nanoparticles that exhibit various colors on the basis of their localized surface plasmon resonance (LSPR). The effects of step-voltage parameters on the coloration of the Ag deposition-based electrochromic device were investigated. Further, we report the use of graphene conductive ink (GCI)/poly(lactic acid) (PLA) as the transparent conductive electrode (TCE). Biopolymer film was coated with graphene ink by spin coating method. The samples were characterized by Fourier transform infrared spectroscopy (FT-IR), X-ray diffractometer (XRD), energy dispersive spectroscopy (EDS), electrical resistance measurements, cyclic voltammetry (CV) and ultraviolet-visible (UV-Vis) spectroscopy. Our results primarily indicate that the novel configuration (PLA/GCI/Ag/GCI/PLA) presents an easy and expeditious way of preparing the multicolor electrochromic device.

(Received January 15, 2018; accepted August 9, 2018)

Keywords: Electrochromic device, Graphene conductive ink, Poly(lactic acid), Silver nanoparticles

1. Introduction

Electrochromic thin films show reversible and persistent changes of their optical properties under charge insertion/extraction [1] and have many applications in contemporary technology such as for energy saving and comfort-enhancing "smart" windows and glass facades in buildings [2,3], high-performance information displays [4,5], "anti-dazzling" rear-view mirrors for cars [6,7], variable-emittance surfaces for thermal control [8,9], etc. Multicolor electrochromism systems, displaying more than two different colors in a single cell, have attracted attention because they have the potential to improve the resolution and color quality in full color electrochromism displays [10,11]. However, most of the inorganic electrochromic materials exhibit only a single color change, and in most case, inorganic electrochromic materials exhibit darkened and cold colors [6,12]. A system that enables control of multichromatic states using only one type of electrochromic material has rarely been reported [13,14].

In order to obtain reversible changes among multiple colors by controlling the localized surface plasmon resonance (LSPR) band, the "voltage-step method" was utilized in a silver (Ag)-deposition-based electrochromic device. This method is based on the application of two consecutive different voltages. Therefore, growth of the Ag nanoparticles and, hence, the color of the electrochromic device are finely controlled by the voltages (-4.2 to +4.0 V) and application time [15]. Ag nanoparticles exhibit various optical states based on their LSPR, and thus they have attracted much attention for surface-enhanced Raman scattering [16], optical sensors [17], photovoltaic [18,19] and electrochromic applications [20].

Graphene has been a highlighted material in the past few years due to its exceptional properties. Many applications of graphenes, such as nanoscale molecular electronics, sensing devices, membranes for gas separation and hydrogen storage, have been reported. Graphene conductive ink (GCI) is of particular interest due to its advantages of being processed in solution which facilitates the low-cost development of electronic and optical devices [21]. The conductive ink is based on the oxygen free graphene ink. The compositions of GCI are 30-40 wt% conductive polymer, 5-15 wt% ethanol, 2-10 wt% diethylene glycol, and <1 wt% graphene. With the oxygen free graphene components, it will increase 5-7 times of the conductivity from the normal base polymer ink. Due to the quick evaporation of the solvent, the resulting dark solution (graphene ink) is easily coated on substrates (polymer and glass) than chemical vapour deposition (CVD) graphene [22].

In our work, the GCI was then coated on the poly(lactic acid) (PLA) supports for the use as a transparent conductive electrode (TCE). The fabrication

and evaluation of a prototype of the novel multicolor electrochromic device based on Ag nanoparticles structure with the following configuration: i.e. PLA/GCI/Ag/GCI/PLA was also described.

2. Experimental details

2.1. Materials

GCI (30-40 wt% conductive polymer, <1 wt% graphene) was obtained from Innophene Company Limited, Thailand. Silver nitrate ($AgNO_3$) was purchased from VWR Chemical Co., USA. PLA film (Grade 4043D, cast sheet co-extrusion, National Metal and Materials Technology Center (MTEC), Thailand) was used as a biopolymer substrate of multicolor electrochromic device. All chemicals used were analytical grade reagents.

2.2. Preparation of GCI coated PLA transparent electrode

PLA film was coated with GCI by spin coating method as follows: 0.5 mL GCI was placed on a 3 cm x 3 cm polymer substrate. PLA film was coated with graphene ink by spin coating at 700 rpm for 35 s. The resulting graphene ink-based coating layer had a very uniform thickness (~10 μm). The PLA film coated with GCI was then dried at 70 ^{o}C for 5 min.

2.3. Multicolor electrochromic device assembly

The synthesis of gel electrolyte for the electrochromic cell was prepared according to the work reported by A. Tsuboi et al. [14]. Fig. 1 represents schematic presentation of the multicolor electrochromic device. It consists of 3 layers: (1) PLA biopolymer substrate, (2) GCI-based transparent conductive electrode, and (3) gel electrolyte and electrochromic active layer. With GCI coated PLA, the electrochromic devices would have lower cost than indium tin oxide (ITO) coated glass slide.

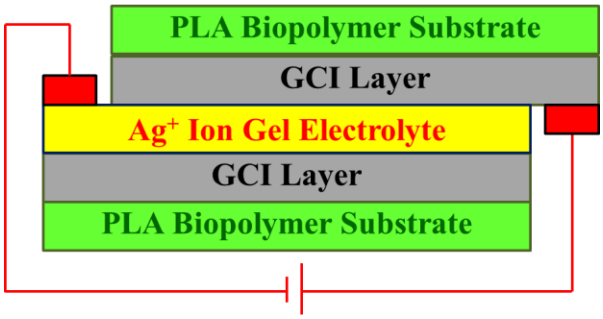

Fig. 1. Schematic diagram of multicolor electrochromic device consisting of Ag^+ ion gel electrolyte

2.4. Materials characterization

The presence of various functional groups in the samples was measured using Fourier transform infrared (FT-IR) spectrometer (Model: Bruker Optics, Vertex70, Germany). Crystallographic information on the samples was obtained using a powder X-ray diffractometer (XRD, LabX XRD-6100, Shimadzu, Japan) with Ge(1 1 1) monochromatized CuKα radiation (λ = 1.542 Å) having a scanning speed of 2°/min. Diffraction data were collected over the 2θ range from 5 to 40°. The energy dispersive spectroscopy (EDS) was used to determine the element composition of manually chosen areas in the samples. The electrical characterization of GCI coated on PLA film was measured by four-point probe technique (S-302-4, Lucas Labs, Canada). Five measurements were performed on different areas of sample to ensure reproducibility. All electrochemistry was performed using a PGSTAT 101 Potentiostat/Galvanostat (Metrohm Autolab B.V., Netherlands) for cyclic voltammetry (CV) analysis. Ultraviolet-visible (UV-Vis) transmission spectra were recorded by using an UV-Vis spectrophotometer (Shimadzu UV-1800, Japan) with a cubic quartz cuvette. The transmittance spectra at the wavelength of 400-700 nm were carried out during CV processing.

3. Results and discussion

The FT-IR spectra of neat PLA and PLA/GCI are shown in Fig. 2. PLA showed typical peaks at 2950, 1750, 1456, 1381 and 1188 cm^{-1}. When GCI (30-40 wt% poly (3,4-ethylenedioxythiophene) (PEDOT) and polystyrene sulfonate (PSS)) was coated on PLA matrix, new peaks appeared at 3273, 1634, and 1264 cm^{-1}, which were assigned to the conformation of conductive polymer. The characteristic bands of graphene at 3450, 1793 and 1641 cm^{-1} are assigned to –OH stretching vibrations, C=C stretching of the benzenoid rings and –Ph, respectively [23]. An increase in the peak intensity usually means an increase in the amount (per unit volume) of the functional group associated with the molecular bond. The results indicate that GCI appeared at the surface of the biopolymer film. Additionally, these changes of surface structure would be expected to facilitate the interaction between conductive layer and polymer matrix [24].

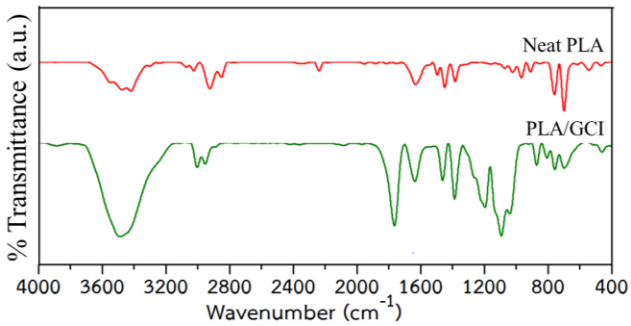

Fig. 2. FT-IR spectra of neat PLA and PLA/GCI

XRD measurement was performed to evaluate the crystalline structures of samples. The changes induced by GCI in the crystal structure of PLA were analyzed further from the XRD patterns of PLA and PLA/GCI samples given in Fig. 3. The characteristic diffraction peak of GCI appears at 26.19° due to the introduction of functional groups on graphene ink. Different from neat PLA, an exceptionally wide diffraction from 10° to 25° is caused by the scattering of PLA biopolymer matrix [25]. The diffraction peak is shown an amorphous of PLA.

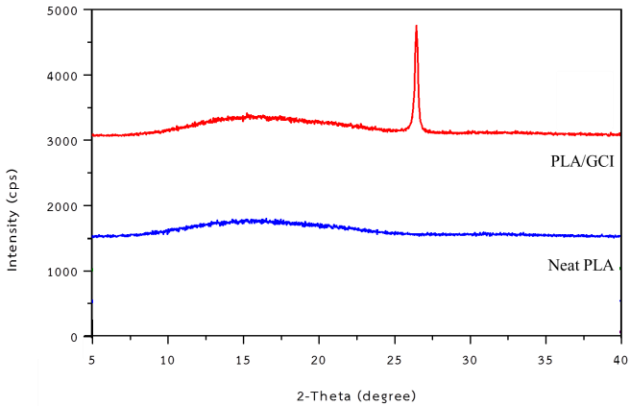

Fig. 3. FT-IR spectra of neat PLA and PLA/GCI

The EDS results of PLA and PLA/GCI were illustrated in Table 1. As shown, the neat biopolymer has a mean carbon (C) contents around 54 at% and an oxygen (O) contents around 44 at%. In the PLA/GCI sample, the C and O contents have mean around 97 and 1 at%, respectively. The remaining 2 at% consists of other elements and impurities, possibly coming from the inadequate purification of raw materials and laboratory (each of them below 0.2 at%). The results indicate that the functional groups of PLA no exist on the surface of PLA/GCI sample.

Table 2 shows the sheet resistance of neat PLA and PLA/GCI. PLA has excellent electrical insulation properties at temperatures ranging from room temperature to around 70 ^{o}C. At temperatures higher than 70 ^{o}C, however, the insulation performance of PLA deteriorates due to its poor heat resistance [26]. The values of sheet resistance decreased after the spin coating of GCI and when the number of cycles is increased. The electrical conductivity of all materials depends on the density; denser materials have higher electrical conductivity. In addition, the number of times a film is spin-coated results in a significant and controllable change in sheet resistance [21]. Based on the electrical resistance measurements, 3 cycles of drop-coating (17 Ω/sq) were selectively performed throughout the experiment.

Table 1. EDS results of neat PLA and PLA/GCI

Sample	Element content (at%)		
	Carbon (C)	Oxygen (O)	Other elements
Neat PLA	54.33	44.07	1.60
PLA/GCI	97.08	1.02	1.90

Table 2. Sheet resistance of neat PLA and PLA/GCI

Sample	Neat PLA	PLA/GCI		
		1 cycle	2 cycles	3 cycles
Sheet resistance (Ω/sq)	Not Detected (Insulator)	109	38	17

The electrochromic device investigated is a cell with two GCI/PLA transparent conductive electrodes sandwiching a Ag^{+} ion gel electrolyte. Fig. 4 shows the cyclic voltammogram for this novel device. As the voltage was scanned from 0 V in the negative direction, an apparent cathodic current was observed from -1.1 V. This current can be attributed to the current used to electrochemically reduce the Ag^{+} dissolved in the gel electrolyte. When the voltage was swept from -2.5 V in a positive direction, the cathodic current disappeared at -1.0 V. The cathodic current observed is due to the growth of the Ag particles. On the other hand, as the voltage was swept in a more positive direction, an anodic current appeared beginning at -0.8 V. This anodic current reflects the oxidation of the electrodeposited Ag [15,20]. These changes in the hysteresis current were all reversible. The current change was stably maintained even after 20 test cycles. As a preliminary repetition stability test, we confirmed stable current changes between cathodic and anodic over 20 cycles of voltage application.

The novel PLA/GCI/Ag/GCI/PLA electrochromic device can be switched from the transparent state (before step voltage application) to the black state (step voltage application -4.0 V for 1 s) and yellow state (step voltage application -4.0 V for 1 s and -1.6 V for 7 s). Both colored states returned to transparent state following application of the oxidation voltage for electrodeposited Ag (+0.5 V). Therefore, changes between the transparent state and each colored state were reversible. Furthermore, when Ag nanoparticles were electrodeposited uniformly on the PLA/GCI transparent conductive electrode using the voltage-step method described above, the electrochromic

device turned black or yellow depending on the time and step voltage application (Fig. 5). All optical changes in this device are based on the same mechanism of Ag deposition. Ag nanoparticles have the ability to interact with visible light through LSPR effects. Furthermore, the optical properties of Ag nanoparticles are affected by their sizes and shapes [14]. Therefore, this method of applying two different voltages is expected to be effective for producing Ag nanoparticles with controlled size and shape and actualizing clear multicolor representation in LSPR-based electrochromic devices.

In transparent state, the optical transmittance at λ = 633 nm for PLA/GCI/Ag/GCI/PLA electrochromic device is 48.03%, while this value in 2 colored states are 5.62 and 34.13%. The decrease of optical transmittance in colored state is achieved by increasing the size of Ag nanoparticles in smart film due to LSPR effect [27]. The optical transmittance differences (ΔT) are calculated between colored and bleached modes at wavelength of 633 nm in each sample. The obtained values for ΔT are reported in Fig. 6 and are equal to 13.89, 28.51 and 42.40%. The response times for bleached and 2 colored states are considered as 0.95 s/6.90 s. Similar results were found in earlier works [14,15,20,27,28]. Coloration efficiency is recognized as a key criterion for measuring and comparing the performance of an electrochromic behavior of an electrochromic device. The use of this novel configuration can be used in smart windows with high coloration efficiency and acceptable switching time.

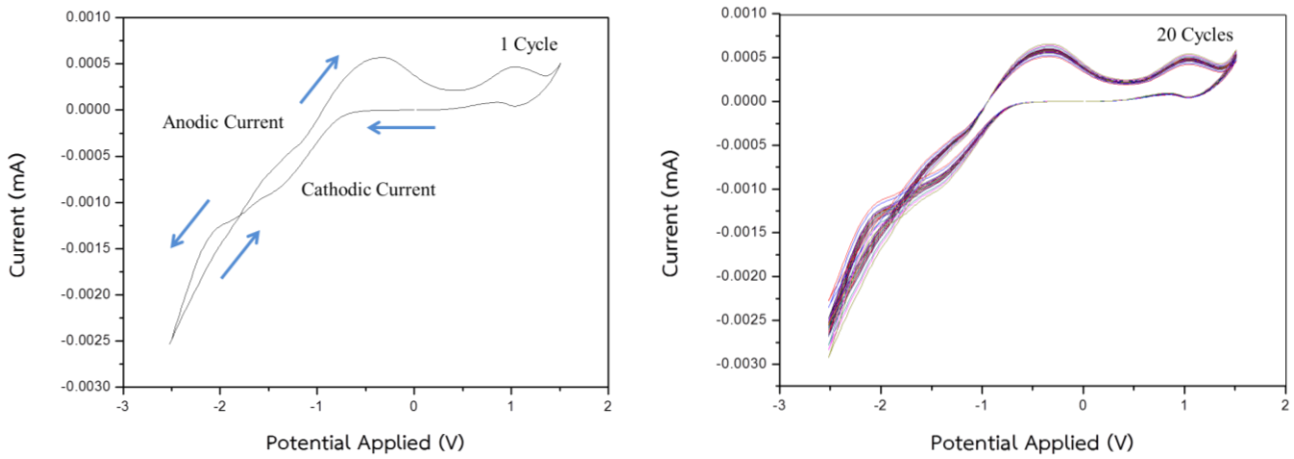

Fig. 4. Cyclic voltammogram of the novel PLA/GCI/Ag/GCI/PLA electrochromic device at 1 cycle and 20 cycles

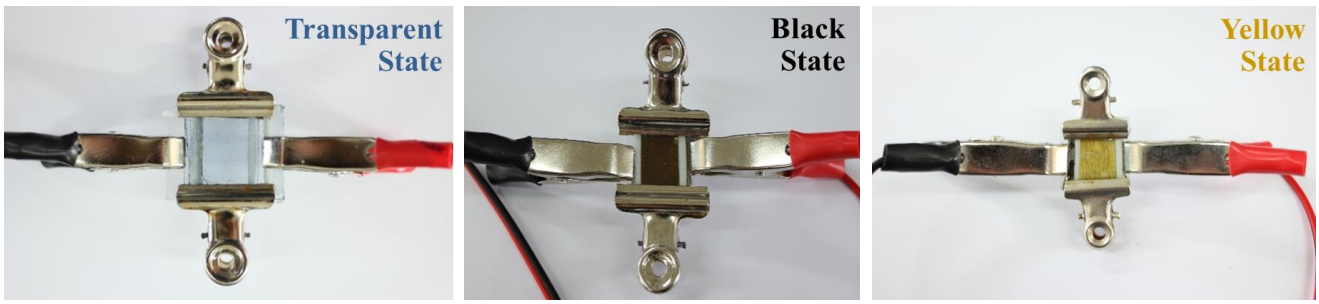

Fig. 5. Photographs of the PLA/GCI/Ag/PLA/GCI electrochromic device showing different colors at different step voltages application: transparent state, black state, and yellow state

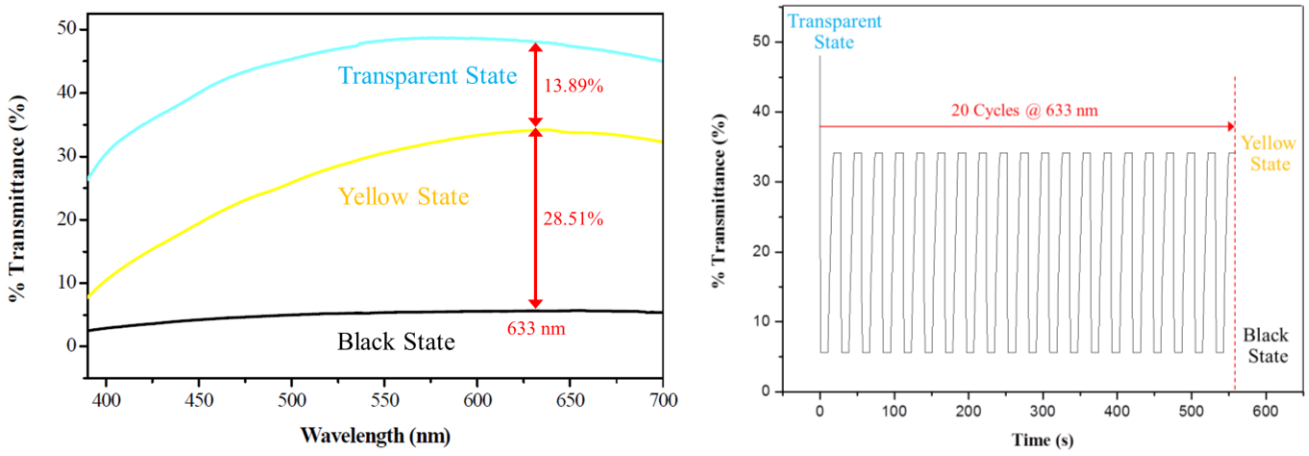

Fig. 6. UV-Vis spectra of the PLA/GCI/Ag/PLA/GCI electrochromic device showing different %transmittance at different step voltages application: transparent state, black state, and yellow state. Response times of multicolor electrochromic device in transparent state and 2 colored states between -4.0 V and -1.6 V switched voltages at λ = 633 nm for 20 cycles

This novel configuration presented an easy, expeditious and green way of preparing electrochromic device. It was fabricated using a single-layer gel electrolyte. The GCI coated on PLA in the electrochromic device demonstrated a potential for replacing ITO coated glass slide in smart windows. The demand for polymer based electrochromic device is increasing in recent years due to not only the advantages of conjugated electrochromic polymers such as high color versatility, large optical contrasts, but also their potential applications in flexible devices [29]. Therefore, we can expect more attempts for the commercialization of polymer-based electrochromic devices in the near future.

4. Conclusions

In this study, the PLA/GCI transparent conductive electrode was used as the supporting electrode of Ag multicolor electrochromic device for the first time. In addition, the effects of step-voltage application on the coloration of the Ag deposition-based electrochromic cell were investigated. The electrochromic device turned black or yellow depending on the time and step voltage application. Both colored states returned to transparent state following application of the oxidation voltage for electrodeposited Ag. Furthermore, the current change was stably maintained even after 20 test cycles. In particular, a significant optical modulation (48.03%, 5.62 and 34.13%) at 633 nm, fast switching speed (0.95 s/6.90 s) for colored-bleached states and high coloration efficiency are achieved for samples. Overall, this novel configuration presented an easy, expeditious and green way of preparing environment-friendly multicolor electrochromic devices and smart windows.

Acknowledgements

This work is supported by Silpakorn University Research and Development Institute. The authors also wish to thank Department of Materials Science and Engineering, Faculty of Engineering and Industrial Technology, Silpakorn University and Center of Excellence on Petrochemical and Materials Technology, Chulalongkorn University for supporting and encouraging this investigation.

Author contributions

All the authors contributed to this work. Assoc. Prof. Achanai Buasri designed the study, conceived the experiments, and wrote the first draft of the paper. Mr. Suparak Ojchariyakul, Ms. Patinya Kaewmanechai, and Ms. Waratchaya Eakviriyapichat performed the experiences in the laboratory. Asst. Prof. Dr. Vorrada Loryuenyong contributed to the conceptual approach, analyzed the data, helped in the discussion of results and thoroughly revised the paper.

Conflict of interest

The authors declare that there is no conflict of interests regarding the publication of this article.

References

[1] R. T. Wen, G. A. Niklasson, C. G. Granqvist, Solar Energy Materials & Solar Cells **120**, 151 (2014).
[2] R. Baetens, B. P. Jelle, A. Gustavsen, Solar Energy Materials & Solar Cells **94**, 87 (2010).
[3] C. G. Granqvist, Solar Energy Materials & Solar Cells **99**, 1 (2012).

[4] V. Rai, N. Tiwari, M. Rajput, S. M. Joshi, A. C. Nguyen, N. Mathews, Electrochimica Acta **255**, 63 (2017).
[5] R. J. Mortimer, A. L. Dyer, J. R. Reynolds, Displays **27**, 2 (2006).
[6] C. G. Granqvist, Thin Solid Films **564**, 1 (2014).
[7] H. N. Cui, M. F. Costa, V. Teixeira, I. Porqueras, E. Bertran, Surface Science **532-535**, 1127 (2003).
[8] Y. He, Y. Xiong, J. Qiu, M. Xu, J. Wang, C. Wu, Y. Zhao, Physics Procedia **18**, 61 (2011).
[9] Y. Fang, P. C. Eames, Energy Conversion and Management **47**, 3602 (2006).
[10] K. Imaizumi, Y. Watanabe, K. Nakamura, T. Omatsu, N. Kobayashi, Physical Chemistry Chemical Physics **13**, 11838 (2011).
[11] K. Wang, T. Zhang, Y. Hu, W. Yang, Y. Shi, Electrochimica Acta **130**, 46 (2014).
[12] K. Wang, T. Zhang, Y. Hu, W. Yang, Y. Shi, Solar Energy Materials & Solar Cells **54**, 147 (1998).
[13] Y. Pang, Q. Chen, X. Shen, L. Tang, H. Qian, Thin Solid Films **518**, 1920 (2010).
[14] A. Tsuboi, K. Nakamura, N. Kobayashi, Solar Energy Materials & Solar Cells **145**, 16 (2016).
[15] A. Tsuboi, K. Nakamura, N. Kobayashi, Chemistry of Materials **26**, 6477 (2014).
[16] K. Kneipp, H. Kneipp, I. Itzkan, R. R. Dasari, M. S. Feld, Journal of Physics: Condensed Matter **14**, R597 (2002).
[17] A. D. McFarland, R. P. Van Duyne, Nano Letters **3**, 1057 (2003).
[18] B. P. Rand, P. Peumans, S. R. Forrest, Journal of Applied Physics **96**, 7519 (2004).
[19] F. Hallermann, C. Rockstuhl, S. Fahr, G. Seifert, S. Wackerow, H. Graener, G. V. Plessen, F. Lederer, Physica Status Solidi (A) - Applications and Materials Science **205**, 2844 (2008).
[20] A. Tsuboi, K. Nakamura, N. Kobayashi, Advanced Materials **25**, 3197 (2013).
[21] A. Buasri, D. Ongmali, P. Sriboonpeng, S. Prompanut, V. Loryuenyong, Key Engineering Materials **744**, 463 (2017).
[22] X. Han, Y. Chen, H. Zhu, C. Preston, J. Wan, Z. Fang, L. Hu, Nanotechnology **24**, 205304 (2013).
[23] Y. Jin, M. Jia, M. Zhang, Q. Wen, Applied Surface Science **264**, 787 (2013).
[24] A. Buasri, N. Chaiyut, V. Loryuenyong, N. Jaritkaun, T. Yavilas, N. Yooruengdech, Optoelectron. Adv. Mat. **7**, 938 (2013).
[25] B. W. Chieng, N. A. Ibrahim, W. M. Z. W. Yunus, M. Z. Hussein, Y. Y. Then, Y. Y. Loo, Polymers **6**, 2232 (2014).
[26] T. Oi, K. Shinyama, S. Fujita, IEEJ Transactions on Fundamentals and Materials **131**, 395 (2011).
[27] H. Najafi-Ashtiani, S. Gholipour, A. Rahdar, Journal of Molecular Structure **1169**, 25 (2018).
[28] A. Buasri, S. Ojchariyakul, P. Kaewmanechai, W. Eakviriyapichat, V. Loryuenyong, Materials Science Forum **926**, 79 (2018).
[29] H. Wang, M. Barrett, B. Duane, J. Gu, F. Zenhausern, Materials Science & Engineering B **228**, 167 (2018).

*Corresponding author: achanai130@gmail.com
vorrada@gmail.com